Repositorio Institucional de la Universidad Autónoma de Madrid

https://repositorio.uam.es

Esta es la **versión de autor** del artículo publicado en:
This is an **author produced version** of a paper published in:

Journal of Physics: Condensed Matter 24.15 (2012): 155303

DOI: http://dx.doi.org/10.1088/0953-8984/24/15/155303

Copyright: © 2012 IOP Publishing

El acceso a la versión del editor puede requerir la suscripción del recurso
Access to the published version may require subscription

Enhanced dielectric constant resolution of thin insulating films by Electrostatic Force Microscopy

E. Castellano-Hernández[1], J. Moreno-Llorena[1], J. J. Sáenz[2] and G. M. Sacha[1]

[1]Departamento de Ingeniería Informática. Universidad Autónoma de Madrid. Campus de Cantoblanco, 28049 Madrid, Spain.

[2]Departamento de Física de la Materia Condensada e "Instituto Nicolás Cabrera". Universidad Autónoma de Madrid. Campus de Cantoblanco, 28049 Madrid, Spain

Email: sacha.gomez@uam.es

Abstract: Electrostatic Force Microscopy has been shown to be a useful tool to determine the dielectric constant of insulating films of nanometer thicknesses that play a key role in many electrical, optical and biological phenomena. Previous approaches make use of simple analytical formulae to analyse the experimental data for thin insulating films deposited directly on a metallic substrate. Here we show that the sensitivity of the EFM signal to changes in the dielectric constant of the thin film can be enhanced by using dielectric substrates with low dielectric constants. We present detailed numerical calculations of the tip-sample electrostatic interaction in the following set-up: the insulating thin film, a dielectric substrate (or spacing layer) of known low dielectric constant and a metallic electrode. The EFM sensitivity to the dielectric constant increases with the thickness of the spacing layer and saturates for thicknesses above 100-300 nm, when it is close to that of an infinite medium.

PACS: 07.79.-v, 81.07.-b, 61.46.-w

Submitted to Journal of Physics: Condensed Matter

1. Introduction

Understanding the electric field distribution in nanostructured thin films is a key issue in nanoscience nowadays.[1] By applying a voltage between a force microscope tip and a sample, electrostatic force microscopy (EFM)[2,3,4,5,6,7,8,9] has been used to analyze different properties of thin films[10,11] at the nanoscale.[12] EFM is currently used to determine the static dielectric constants of thin films of a few nanometers thickness directly deposited on a metallic electrode. The dielectric constant can be determined by comparison of the experimental results with simple analytical expressions[13,14,15]. For metallic samples, the tip-sample interaction is very well understood and the force, as well as the force gradient, can be determined by using a simple analytical model.[13] The tip-sample interaction due to the thin film dielectric response can be considered as a perturbation of the reference system in absence of the thin film. In contrast with metallic substrates, the electrostatic interactions with dielectric samples depend on the macroscopic geometry of the tip-sample system and, although it is possible to compute it numerically[16], no simple closed expressions are available.

In this article, we analyze the effect of the experimental parameters of a sample composed by two dielectric layers (thin film and substrate) over a metallic plate. First, we develop a numerical method that is able to accurately calculate the electrostatic interaction between such as structure and an EFM tip. Focusing on the thin film dielectric constant estimation, we analyze the capability of the EFM (dielectric contrast)[17,18,19], using both the electrostatic force F and force gradient G, as a function of the thin film thickness, sample dielectric constant and metallic plate distance. As we will show, the EFM sensitivity to changes of the dielectric constant of a thin dielectric film can be greatly enhanced when the film is deposited on a low dielectric constant substrate.

2. Theoretical Background

In a typical EFM setup, we have a metallic tip connected to a battery that applies a constant electric potential V_0. The tip is placed over a sample at a tip-sample distance D. The tip is characterized by three geometrical parameters: The apex radius R_{tip}, the half-angle θ and the length L. To solve electrostatic problems with this geometry, an algorithm called the Generalized Image Charge Method[13,20] (GICM) has been developed. The

GICM replaces the surface charge density by a set of charges inside the metallic tip. The q_i charge values are obtained by a standard least-squares minimization. Its efficiency has been demonstrated for systems where the sample includes objects such as Carbon Nanotubes[21] or graphene[22]. In all of these cases, the influence of the sample has been included in the minimization by a set of image charges.

In the case of a thin film, the sample is composed by three layers: 1) a dielectric thin film with dielectric constant ε_1 and thickness h_1; 2) a dielectric substrate with dielectric constant ε_2 and thickness h_2 and 3) a grounded metallic plate below the surface (see Figure 1). The image charges of such as structure are obtained by solving the Laplace/Poisson equation in cylindrical coordinates (z,ρ,ϕ). In general, for every dielectric region of the sample, the electrostatic potential V_i can be written as

$$V_i = \frac{qi}{4\pi\varepsilon_0}\left[\int_0^\infty \mathrm{J}_0(\mathrm{k}\rho)(\psi_i(\mathrm{k})\mathrm{e}^{-\mathrm{Kz}} + \theta_i(\mathrm{k})\mathrm{e}^{\mathrm{Kz}})\mathrm{dk}\right] \quad (1)$$

where ψ_i and θ_i are a set of coefficients that are obtained by applying the electrostatic boundary conditions ($V_i=V_{i+1}$ and $\varepsilon_i V'_i=\varepsilon_{i+1}V'_{i+1}$ where V is evaluated at the interface between regions i and i+1, i.e. $z_{i,i+1}$) to the sample interfaces. In the case of the three layers sample, the coefficients take the following form (see figure 1 for a graphic description of the three layers):

$$\widetilde{H}\theta_0(K) = (C_{12} - e^{-2Kh_2})e^{-2Kz_{12}} - C_1(1 - C_{12}e^{-2Kh_2})e^{-2Kz_{01}} \quad (2)$$

$$\widetilde{H}\theta_1(K) = \frac{2(C_{12} - e^{-2Kh_2})}{\varepsilon_1+1}e^{-2Kz_{12}} \quad (3)$$

$$\widetilde{H}\psi_1(K) = \frac{2}{\varepsilon_1+1}(1 - C_{12}e^{-2Kh_2}) \quad (4)$$

$$\widetilde{H}\psi_2(K) = \frac{4\varepsilon_1}{(\varepsilon_1+1)(\varepsilon_1+\varepsilon_2)} \quad (5)$$

$$\widetilde{H}\theta_2(K) = \frac{4\varepsilon_1 e^{-2Kz_{23}}}{(\varepsilon_1+1)(\varepsilon_1+\varepsilon_2)} \quad (6)$$

where

$$\widetilde{H} = 1 - C_{12}C_1e^{-2Kh_1} - (C_{12} - C_1e^{-2Kh_1})e^{-2Kh_2} \quad (7)$$

and $C_1=(\varepsilon_1-1)/(\varepsilon_1+1)$; $C_{12}=(\varepsilon_1-\varepsilon_2)/(\varepsilon_1+\varepsilon_2)$. Once the coefficients have been obtained, Eq. (1) can be used to include the thin film and sample in the GICM minimization routine. Once we know the coefficients, we are able to solve the problem and obtain the electrostatic potential by direct integration of equation 1. The electrostatic

potential can be also written as a sum of image charges by applying $(1+x)^{-1}=\Sigma(-x)^n$ (only valid when $-1<x<1$) to $\widetilde{H}^{-1}$. In the general case, $\widetilde{H}^{-1}$ takes the following form:

$$\widetilde{H}^{-1} = \sum_{n=0}^{\infty}(C_{12}C_1)^n\, e^{-2Knh_1}\left[1+\sum_{i=1}^{n}\binom{n}{i}(C_1)^{-i}\, e^{-2Ki(h_2-h_1)}\left(1+\sum_{j=1}^{i}\binom{i}{j}(-\frac{C_1}{C_{12}})^j\, e^{-2Kjh_1}\right)\right] \qquad (8)$$

Combining equation 1 and 8, we obtain three different series that comes from the three sums in equation 8. The first problem we find is that, in the case of $\widetilde{H}$, the condition $-1<x<1$ is not always truth. However, it is easy to demonstrate that the system fits this condition in the limit $\varepsilon_1 > \varepsilon_2$. This condition will be found in most of the systems since the opposite limit ($\varepsilon_1 > \varepsilon_2$) usually corresponds to the case where the substrate below the thin film is a metal and can be analysed by previous methods[13]. The second and most important problem is that the three series depend on each other and there is not a simple way to express them. We have found that, depending on the geometry of the sample, the sums can be combined in different ways to improve the performance of the computational simulations. However, in the limit $h_2\rightarrow\infty$, $\widetilde{H}^{-1}$ takes the following form:

$$\widetilde{H}^{-1} = \sum_{n=0}^{\infty}(C_{12}C_1)^n\, e^{-2Knh_1} \qquad (9)$$

In this case, the condition $-1<x<1$ is valid for every possible value of C_{12}, C_1 and h. Combining equations 1 to 8 and 9 we can finally show the electrostatic potential as follows:

$$V_1 = \frac{q}{4\pi\varepsilon_0}\left[\frac{1}{\sqrt{\rho^2+(z-z_m)^2}} - \frac{C_1}{\sqrt{\rho^2+(z+z_m)^2}} + \frac{4C_{12}\varepsilon_1}{(\varepsilon_1+1)^2}\sum_{n=0}^{\infty}\frac{(C_{12}C_1)^n}{\sqrt{\rho^2+[z+z_m+2h_1(n+1)]^2}}\right] \qquad (10)$$

$$V_2 = \frac{q}{4\pi\varepsilon_0}\frac{2}{(\varepsilon_1+1)}\sum_{n=0}^{\infty}(C_{12}C_1)^n\left[\frac{1}{\sqrt{\rho^2+(z-z_m-2nh_1)^2}} + \frac{C_{12}}{\sqrt{\rho^2+[z+z_m+2h_1(n+1)]^2}}\right] \qquad (11)$$

$$V_3 = \frac{q}{4\pi\varepsilon_0}\frac{4\varepsilon_1}{(\varepsilon_1+1)(\varepsilon_1+\varepsilon_2)}\sum_{n=0}^{\infty}(C_{12}C_1)^n\frac{1}{\sqrt{\rho^2+(z-z_m-2nh_1)^2}} \qquad (12)$$

Where z_m is the distance between the punctual charge and the thin film surface.

One of the advantages of this formalism is that we can calculate the electrostatic force between the punctual charge and the sample by the interaction between the charge itself and the image charges obtained from V_1. Another advantage is that we can develop expressions for the interaction between different charged elements such as linear charges by getting the value and position of the image charges from equations 10, 11 and 12. In

the limit $h_2 \to \infty$, Eq. (1) can be written as an infinite series of image charges. In this case, the electrostatic potential at the tip region can be written as $V=V_q+V_{\varepsilon 1,\infty}+V_{tf}$ where V_q is the potential of the punctual charge, $V_{\varepsilon 1,\infty}$ is the image charge of a semiinfinite dielectric plane with $\varepsilon=\varepsilon_1$ and V_{tf} is

$$V_{tf} = \frac{q}{4\pi\varepsilon_0}\frac{4C_{12}\varepsilon_1}{(\varepsilon_1+1)^2}\sum_{n=0}^{\infty}\frac{(C_{12}C_1)^n}{\sqrt{\rho^2+[z+z_m+2h_1(n+1)]^2}} \quad (13)$$

where $C_1=(\varepsilon_1-1)/(\varepsilon_1+1)$, $C_{12}=(\varepsilon_1-\varepsilon_2)/(\varepsilon_1+\varepsilon_2)$. Figure 1 shows an equipotential distribution of a typical EFM tip over the three layers sample.

3. **Effect of the thin film thickness and substrate dielectric constant**

Our main goal is to determine the dielectric constant of the thin film assuming we know the rest of the system parameters. We have used an EFM tip described by V_0=1V, R_{tip}=25nm, θ=17.5º and L=14µm at a tip-sample distance D=5nm (a typical EFM working distance). Let us define ε_{11} and ε_{12} as the ε_1 values that must be distinguished. In Figure 2 we show the electrostatic force as a function of ε_1 for different h_1 values. The capability of the EFM to discriminate two ε_1 values depends on the difference between $F(\varepsilon_{11})$ and $F(\varepsilon_{12})$. To measure it, we define R[F] as the difference between $F(\varepsilon_{11})$ and $F(\varepsilon_{12})$ normalized to their average value $\overline{F}$:

$$R[F] = \frac{2|F(\varepsilon_{11})-F(\varepsilon_{12})|}{|F(\varepsilon_{11})+F(\varepsilon_{12})|} \quad (14)$$

R[F] can be also defined for the gradient force by changing F to G in Eq. (14) (i.e. R=R[G]). Figure 3 shows R[F] and R[G] as a function of ε_2 and h_1 in the limit $h_2 \to \infty$. For any h_1, both R[F] and R[G] increases when ε_2 decreases. We can establish that low ε_2 values are a good choice for getting high contrast values. On the other side, focusing on the dependence of R[F] and R[G] with h_1, we find that it is not uniform. Although, in general, R[F] and R[G] increases when h_1 increases, we must take care of the limit of small ε_2 values (<4) and big h_1 values (>100nm). In this case, both R[F] and R[G] decrease when h_1 increases. For example, when ε_2=2, R[F]($h_1 \to \infty$)=42,75% and R[F](h_1=1µm)=45.21%. It is worth noting that R[F] is still much smaller when h_1 is small (R[F] (h_1=1nm)=5.85%). As we can see in the insets of Figure 3, in the limit $\varepsilon_2 \to 1$, both R[F] and R[G] decreases when h_1 increases.

Another point that must be taken into account is the negative effect of reducing ε_2 on the absolute value of F and G. As we can see in figure 4, both |F| and |G| strongly decreases when ε_2 decreases. Focusing, for example, on h_1=1nm, we can see that R[F] changes from R[F]=0.9% when ε_2=20 to R[F]=66.25% when ε_2=1. However, the absolute value of F is strongly reduced from ε_2=20 (F=98.6pN) to ε_2=1 (F=0.28pN). This collateral effect can be reduced, for example, by increasing V_0 since both F and G are proportional to V_0^2. On the other side, both R[F] and the absolute value of F increase when h_1 increases (same happens with the gradient force G). As we can see comparing Figure 3(a) and 3(b), the gradient force is a better choice than the electrostatic force since R[G] is always bigger than R[F].

4. Finite dielectric substrate influence

In Figure 5(a) we analyze the effect of h_2 (i.e. the distance of the metallic plate) for different ε_2 and a h_1=2nm. In general, both R[F] and R[G] increase when h_2 increases. However, as we can see in the figure, this effect is very different depending on the measured magnitude and the experimental setup. Focusing on both the gradient force, the effect is only relevant when h_2<300nm. On the other side, h_2 has a strong influence when the measured magnitude is F, especially for small ε_2 values (for ε_2=1, F(tip) does not vanish until D>50μm). To understand this effect, we use the analytical model proposed by Sacha et al[14] for a thin film over a metallic sample. In this case, F can be written as the sum of two independent contributions: $F=-[F_1(L,\theta)+F_2(R_{tip},D,\varepsilon_1,h_1)]$. This approximation is very convenient for our analysis since it isolates the contribution of the macroscopic shape of the tip (L and θ only modifies the first term F_1). Deriving this equation, we obtain $G=dF/dD=-F_2'$. Now we can deduce that R[F] is proportional to $[F_2(\varepsilon_{11})-F_2(\varepsilon_{12})]/[F_1+F_2(\varepsilon_{11})+F_2(\varepsilon_{12})]$ and R[G] is proportional to $[F_2'(\varepsilon_{11})-F_2'(\varepsilon_{12})]/[F_2'(\varepsilon_{11})+F_2'(\varepsilon_{12})]$. In this model, high F_1 values reduces R[F], without making any change to R[G]. The behavior of F_1 is described in Figure 5(b), where we show F as a function of the tip sample distance for a sample where h_2=300nm for both a macroscopic tip F(tip) and a sphere F(sphere) (F_1=0 for spherical tips). As we can see, F(sphere) vanishes at very small tip-sample distances ($D+h_2\approx$300nm), showing that F_1 (i.e. the macroscopic shape of the tip) is the main contribution when $D+h_2 \gg R_{tip}$. Moreover, R[F] is especially affected

by F_1 when ε_2 is small since, in this case, the dielectric substrate cannot block the electric field before it reaches the metallic plate.

5. Conclusions

In conclusion, we have presented detailed numerical calculations of the tip-sample electrostatic interactions in the following set-up: the insulating thin film, a dielectric substrate (or spacing layer) of known low dielectric constant and a metallic electrode. We have shown that the sensitivity of the EFM signal to changes in the dielectric constant of the thin film can be greatly enhanced by using dielectric substrates with low dielectric constants. We have demonstrated that, although placing the thin film over samples with a very low dielectric constant decreases the absolute value of the interaction, the contrast increases. For h_1=1nm, the contrast increases more than 60% from $\varepsilon_2=\infty$ to $\varepsilon_2=1$. On the other side, the thin film thickness is directly proportional to both the contrast and the absolute value of the interaction. Exceptionally, the increasing of the contrast changes its tendency for very low values of the dielectric constant of the sample and high values of the thin film thickness. Focusing on the substrate thickness, the EFM sensitivity to the dielectric constant increases with the thickness of the spacing layer and saturates for thicknesses above 100-300 nm, when it is close to that of an infinite medium.

Acknowledgements

Authors acknowledge C. Gómez-Navarro, J. Gómez-Herrero, P. Varona and F. Rodríguez for insightful discussions. This work was supported by TIN2010-19607, the Spanish MICINN (Grant No: FIS2009 − 13430 −C02 − 02) and by the Comunidad de Madrid Microseres Program (Grant No: S2009/T IC − 1476). GMS acknowledges support from the Spanish Ramón y Cajal Program.

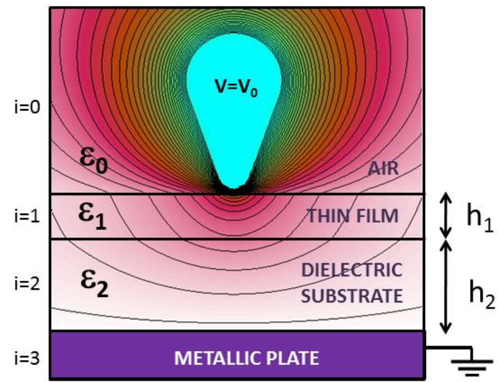

FIGURE 1. Equipotential distribution between an EFM tip and a 3 layers sample: thin film, dielectric substrate and grounded metallic plate. ε_1=20 ε_2=5.

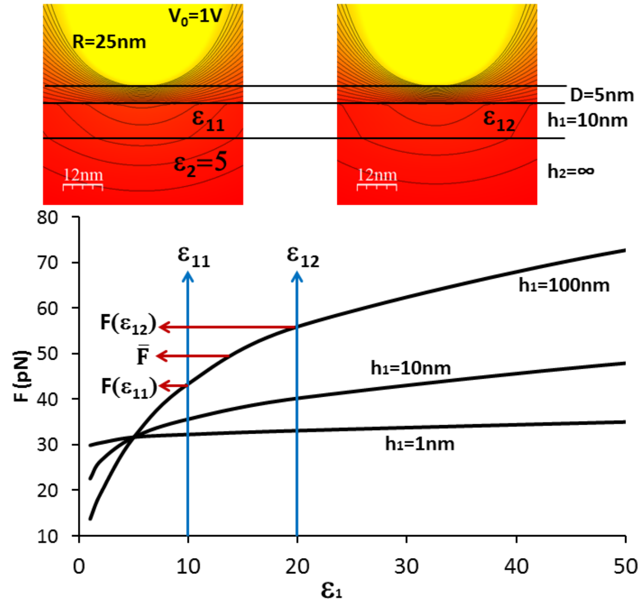

FIGURE 2. Electrostatic force as a function of the thin film dielectric constant for different thin film thicknesses. Equipotential lines are also shown for the two dielectric constant ε_{11} and ε_{12} that must be distinguished and a thickness of 10nm.

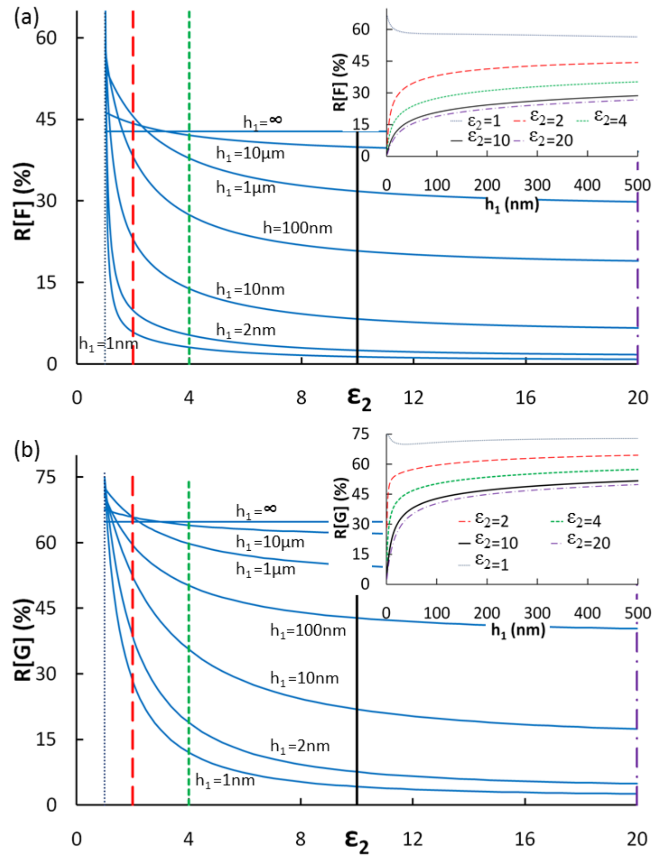

FIGURE 3. R[F] (a) and R[G] (b) as a function of the substrate dielectric sample and the thin film thickness (inset). Vertical lines of the main figure indicates de profiles followed in the inset. $h_2=\infty$. $\varepsilon_{11}=10$, $\varepsilon_{12}=20$. $V_0=1V$. $L=14\mu m$, $\theta=17.5º$, $R_{tip}=25nm$. $D=5nm$.

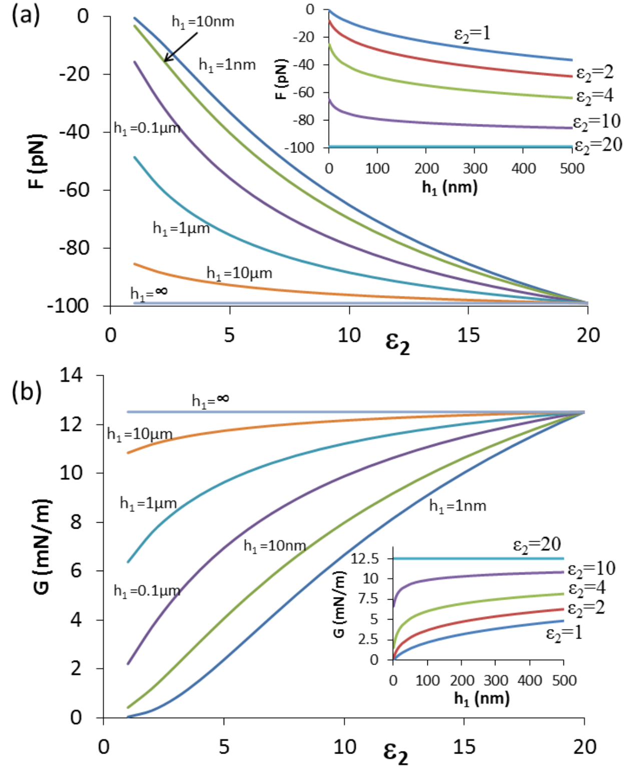

FIGURE 4. (a) Electrostatic force F as a function of the substrate dielectric constant and the thin film thickness (inset). (b) Vertical gradient force as a function of the substrate dielectric constant and the thin film thickness (inset). In both figures we used. $h_2=\infty$. $\varepsilon_1=20$, $V_0=1V$. $L=14\mu m$, $\theta=17.5°$, $R_{tip}=25nm$. $D=5nm$

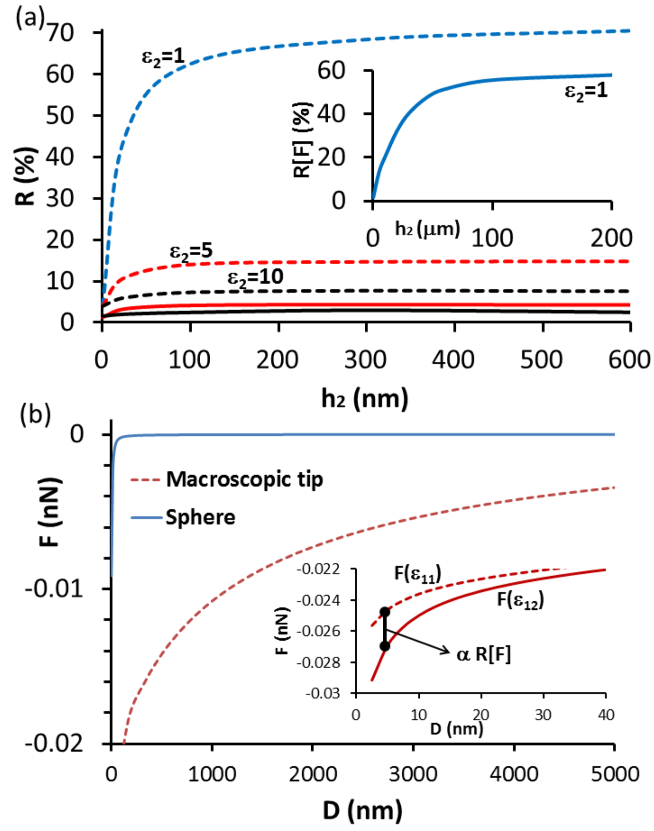

FIGURE 5. (a) R[F] (continuous lines) and R[G] (dashed lines) as a function of the dielectric substrate thickness for different susbtrate dielectric constants. Inset show R[F] when $\varepsilon_2=1$ for a wider scale. D=5nm, h_1=2nm, V_0=1V. (b) Electrostatic force vs tip-sample distance for a sphere and a macroscopic tip. Inset shows the electrostatic force for the two ε_1 values that must be distinguished. As shown in the inset, the distance between $F(\varepsilon_{11})$ and $F(\varepsilon_{12})$ is proportional to the magnitude R[F]..

[1] Vogel E M 2007 *Nat. Nanotechnol*. **2** 25

[2] Kalinin S V, Jesse S, Rodriguez B J, Eliseev E A, Gopalan V and Morozovska A N 2007 *Appl. Phys. Lett*. **90** 212905

[3] Guriyanova S, Golovko D S and Bonaccurso E 2010 *Measurement Science and Technology* **21** 025502

[4] Verdaguer A et al 2009 *Appl. Phys. Lett*. **94** 233105

[5] Schönenberger C and Alvarado S F 1990 *Phys. Rev. Lett.* **65** 3162

[6] Gekhtman D, Zhang Z B, Adderton D, Dresselhaus M S and Dresselhaus G 1999 *Phys. Rev. Lett.* **82** 3887

[7] Palacios-Lidón E, Abellán J, Colchero J, Munuera C and Ocal C 2005 *Appl. Phys. Lett*. **87** 154106

[8] Morozovska A N, Eliseev E A and Kalinin S V 2007 *J. Appl. Phys.* **102** 074105

[9] Krauss T D and Brus L E 1999 *Phys. Rev. Lett.* **83** 4840

[10] McCann E 2006 *Phys. Rev. B.* **74** 161403

[11] Guinea F 2007 *Phys Rev. B.* **75** 235433

[12] Gramse G, Casuso I, Toset J, Fumagalli L and Gomila G 2009 *Nanotechnology* 20 395702

[13] Sacha G M, Sahagún E and Sáenz. J J 2007 *J. Appl. Phys*. **101** 024310

[14] Fumagalli L, Gramse G, Esteban-Ferrer D, Edwards M A and Gomila G 2010 *Appl. Phys. Lett*. **96** 183107

[15] Casuso I, Fumagalli L, Gomila G and Padrós E 2007 *Appl. Phys. Lett*. **91** 063111

[16] Sacha G M, Rodríguez F, Serrano E and Varona P 2010 *JEMWA* **24** 1145

[17] Jacobs H O, Leuchtmann P, Homan O J and Stemmer A 1999 *J. Appl. Phys.* **84** 1168

[18] Sacha G M 2009 *IEEE Transactions on Nanotechnology* **8** 148

[19] Kitamura S and Iwatsuki M 1998. *Appl. Phys. Lett.* **72** 3154

[20] An online version of the GICM is available at www.ii.uam.es/~sacha. A free windows version is also available.

[21] Sacha G M and Sáenz J J 2008 *Phys. Rev. B* **77** 245423

[22] Sacha G M *et al* 2009 *Nanotechnology* **20** 285704